International Journal of Applied Pharmaceutics

ISSN- 0975-7058 Vol 17, Issue 4, 2025

Original Article

IN SILICO DESIGN AND IDENTIFICATION OF POTENTIAL D-ALA: D-ALA LIGASE INHIBITORS AGAINST *STAPHYLOCOCCUS AUREUS*

ABISHA THOMAS, MD. AFZAL AZAM*

Department of Pharmaceutical Chemistry, JSS College of Pharmacy, JSS Academy of Higher Education and Research, Ooty, Nilgiris, Tamil Nadu, India

***Email:** afzal@jssuni.edu.in

Received: 08 Apr 2025, Revised and Accepted: 27 May 2025

ABSTRACT

Objective: This study aimed to identify potent inhibitors of *Staphylococcus aureus D-alanine*: D-alanine ligase (SADDL), a key enzyme in bacterial cell wall synthesis, by designing and evaluating a series of hydrazine carbothioamide derivatives. These scaffolds were selected due to their previously reported antimicrobial activity and potential for structural optimization.

Methods: Nine novel hydrazine carbothioamide derivatives were rationally designed and computationally assessed using an integrated in silico workflow. Molecular docking was performed against the SADDL active site (PDB ID: 2I80) using the Glide module to estimate binding affinity through Glide score, Extra-precision Hydrogen-bonding (XP H-bonding), van der Waals, Coulombic energy, and E-model scores. Binding free energies (ΔG_bind) were calculated using Molecular Mechanics-General Born Surface Area (MM-GBSA) to refine the ranking. To validate stability, a 100 ns Molecular Dynamics (MD) simulation using Desmond was conducted for the top-ranked compound, with Root mean Square Deviation (RMSD), Root mean Square Fluctuation (RMSF), and protein–ligand interaction analysis.

Results: Compound 1 demonstrated the best binding affinity with a Glide score of-11.11 kcal/mol and ΔG_bind of-96.06 kcal/mol, outperforming the co-crystallized ligand (-9.88 kcal/mol and- 59.98 kcal/mol). It exhibited strong van der Waals (-27.87kcal/mol) and Coulombic (-207.11kcal/mol) energies, as well as significant XP H-bonding (-3.25kcal/mol). Compound 6 and 8 also showed favorable interactions. MD simulations confirmed the stable binding of Compound 1 up to 60 ns, with consistent RMSD and low RMSF. Key residues involved included Ser150, Ser151, Glu187, and Lys215. Coordination with Mg^{2+} via Glu270, Asp257, and Ser150 further enhanced binding stability.

Conclusion: Compound 1 emerged as a promising SADDL inhibitor with strong and stable binding, suggesting its potential as a lead antibacterial agent. Further *in vitro* and *in vivo* studies are warranted.

Keywords: SADDL, Molecular docking, MM-GBSA, MD simulation, Glide score, RMSD, Antibacterial agent, *Staphylococcus aureus*, Protein–ligand interaction, Mg^{2+} coordination

DOI: https://dx.doi.org/10.22159/ijap.2025v17i4.54510 Journal homepage: https://innovareacademics.in/journals/index.php/ijap

INTRODUCTION

The continuous rise in bacterial resistance to currently available antibiotics is a serious global health threat, leading to increased rates of illness and death worldwide [1, 2]. This growing concern highlights the urgent requirement for the development of new antibacterial agents that function through novel mechanisms. Among such promising molecular targets is D-alanine: D-alanine Ligase (DDL), an enzyme that plays a critical role in the early stages of bacterial cell wall formation [3, 4]. Specifically, DDL catalyzes an ATP-dependent reaction to produce the D-alanine-D-alanine dipeptide, an essential component of the Uridine diphosphate–N–acetylmuramic–Pentapeptide (UDP-MurNAc-pentapeptide), which serves as a building block for bacterial peptidoglycan layers [5, 6]. Disrupting the activity of this enzyme can interfere with bacterial cell wall biosynthesis, ultimately halting bacterial growth. This makes DDL a well-validated and attractive target for antibacterial drug development [7]. There are two major isoforms of DDL, namely D-alanine--D-alanine Ligase A (DDLA) and D-alanine--D-alanine Ligase B (DDLB), which have been isolated and thoroughly studied in bacteria such as *Escherichia coli* and *Salmonella typhimurium.* These isoforms contribute to essential steps in peptidoglycan biosynthesis and represent viable targets for selective inhibition. In *Staphylococcus aureus* and other Gram-positive bacteria, resistance to glycopeptide antibiotics such as vancomycin often arises through the acquisition of alternate cell wall biosynthesis pathways. These resistance mechanisms are primarily mediated by enzymes that substitute the terminal D-Ala-D-Ala dipeptide with modified versions such as D-Ala-D-Lac or D-Ala-D-Ser, which reduce antibiotic binding affinity. In Vancomycin-Resistant *Enterococci (VRE),* for example, biosynthetic pathways involving the production of D-Ala-D-Lac (encoded by VanA, VanB, VanD) or D-Ala-D-Ser (VanC, VanE, VanG, VanL) are facilitated by specialized ligases [8, 9]. Although *Staphylococcus aureus* typically acquires resistance through the VanA operon, often via horizontal gene transfer, the enzymatic mechanisms underlying these substitutions highlight the critical role of D-Ala-D-Ala Ligases (DDL) and their homologs. Targeting DDL and its isoforms-or even the alternative ligases involved in resistance-therefore presents a promising strategy for the development of broad-spectrum antibacterial agents capable of combating resistant strains [10, 11]. Structural biology has significantly advanced our understanding of DDL, with X-ray crystallography providing detailed insights into the structure of DDLB, both in its native form and in complex with inhibitors. These studies have been fundamental in supporting structure-based drug design approaches [12–17]. In *Staphylococcus aureus,* the DDL enzyme (SADDL) functions as a dimer, with each monomer consisting of a combination of parallel and antiparallel β-sheets surrounded by α-helices. Structurally, the enzyme is organized into three main regions: N-terminal, central, and C-terminal domains. The ATP-binding site is located at the interface between the N-and C-terminal domains, and plays a critical role in the ligation process [18, 19]. Kinetic studies have shown the presence of two distinct D-alanine binding sites, with the N-terminal region having a stronger affinity for the first D-alanine and the C-terminal region engaging the second with less affinity [20]. One well-known inhibitor of DDL is D-cycloserine, a broad-spectrum antibiotic that functions by competitively blocking the enzyme's active site. It has been used clinically in the treatment of tuberculosis [21,]. However, its practical application is limited due to its neurotoxic side effects [22]. To overcome these drawbacks, alternative chemical classes such as phosphonates, and phosphamides have been developed, offering potential as transition-state analogs that mimic the natural enzyme substrates [23–26]. Both experimental and computational methods have been employed

to discover novel DDL inhibitors, with computational tools offering efficient strategies to screen large compound libraries and predict molecular interactions [27].

MATERIALS AND METHODS

Materials

The Schrödinger Suite was employed to carry out various computational studies, including molecular docking, MM-GBSA binding energy calculations, and molecular dynamics simulations. For docking experiments, the crystal structure of SADDL, with PDB ID: 2I80, was retrieved from the Protein Data Bank. Ligand molecules were either designed or sourced, specifically focusing on novel hydrazine carbothioamide-linked derivatives as potential inhibitors.

Molecular docking

To explore the binding interactions between the designed compounds and the SADDL protein (PDB ID: 2I80), molecular docking studies were carried out using the Schrödinger Suite (2021-4) [28]. Ligand structures were prepared using LigPrep, which generated energy-minimized 3D conformations and predicted relevant ionization states and tautomeric forms. The SADDL protein structure (PDB ID: 2I80) was pre-processed using the Protein Preparation Wizard. During this process, accurate protonation states were assigned, non-essential heteroatoms were removed, and crystallographic water molecules were deleted, except for those in proximity to the active site and coordinating the Mg^{2+} ion. These key water molecules were retained due to their potential structural and functional significance in ligand binding and metal ion stabilization, ensuring the integrity of the docking environment [29]. Glide was used to perform the docking simulations. Initially, ligands were docked using Standard Precision (SP) mode, followed by Extra Precision (XP) mode to refine binding poses and improve accuracy [30, 31]. The docking grid was generated to encompass the active site of the SADDL protein, centered on the co-crystallized ligand to ensure accurate targeting. The grid box dimensions were set to 12 Å (X-axis), 13 Å (Y-axis), and 24 Å (Z-axis), effectively covering the ligand-binding pocket and surrounding residues critical for molecular interactions. Docking scores were computed to estimate the binding affinity of each ligand toward the active site of SADDL [32, 33].

MM-GBSA calculations

MM-GBSA calculations were performed using the Prime module of the Schrödinger Suite to estimate the binding free energies of the ligand–protein complexes. This approach integrates molecular mechanics with Generalized Born (GB) solvation models and Solvent-Accessible Surface Area (SASA) calculations to provide a comprehensive prediction of binding affinity. Prior to energy calculations, the complexes were energy-minimized and equilibrated to ensure accuracy. By accounting for solvation effects, electrostatic interactions, and van der Waals forces, the MM-GBSA method delivered a more refined and realistic evaluation of the ligand binding energies [34, 35].

Molecular dynamics simulations

To assess the stability and dynamic behavior of the ligand–SADDL complexes, MD simulations were conducted using the Desmond module within the Schrödinger Suite. Each system was solvated with Transferable Intermolecular Potential with 3 Points (TIP3P) water molecules in an orthorhombic simulation box, and counterions were added to neutralize the overall charge. Following energy minimization, the systems were equilibrated under Number of Particles (NPT) conditions (constant number of particles, pressure, and temperature). A 100-nanosecond production run was performed to monitor the complexes over time. The resulting MD trajectories were analyzed to evaluate binding stability, track conformational fluctuations, and identify key protein–ligand interactions throughout the simulation period [36].

RESULTS

Molecular docking results and analysis

Docking studies were conducted using the catalytic domain of the *Staphylococcus aureus* D-alanine: D-alanine Ligase (SADDL) protein crystal structure (PDB ID: 2I80), employing the Schrödinger Suite 2021-4. Ligands with RMSD values within 1.78 Å were considered well-aligned with the co-crystallized ligand during virtual screening. Lipinski's Rule of Five was applied to eliminate compounds with unfavorable functional groups that could hinder binding interactions. Key Glide XP docking parameters, such as Glide score, e-model, van der Waals energy (E_vdw), Coulomb energy (E_coul), and total docking energy (E_energy)-were assessed to evaluate the docking results thoroughly.

Table 1: The XP-docking scores for the catalytic domain of (SADDL) protein crystal structure (PDB ID: 2I80)

Comp	Glide score kcal/mol	Glide vedw	Glide ecou	Glide energy	Glide emodel	Xp H bond
1	-11.11	-27.87	-207.11	-62.01	-82.76	-3.25
2	-10.38	-8.55	-184.07	-37.48	-34.80	-2.78
3	-10.22	-29.92	-172.03	-51.72	-53.42	-0.75
4	-10.15	-36.37	-137.58	-33.09	-47.24	-0.76
5	-10.08	-14.74	-185.03	-33.02	-38.57	-2.82
6	-10.20	-45.35	-218.46	-51.23	-55.12	-4.18
7	-10.11	-13.54	-165.99	-31.99	-23.28	-1.11
8	-9.67	-44.67	-136.87	-40.15	-49.96	-3.17
9	-9.03	-6.03	-190.73	-32.87	-36.93	-3.15
Co-crystal	-9.88	-37.36	-176.19	-44.56	-62.92	-0.7

[a]Glide Score, [b]Glide E-model, [c]Glide Van der Waals Energy, [d]Glide Coulomb Energy, [e]Glide Energy.

Compound 1 exhibited the most favorable binding affinity, with the lowest Glide score of-11.11 kcal/mol, significantly outperforming the co-crystal ligand (-9.88 kcal/mol). This strong interaction was further supported by its highly negative van der Waals (-27.87 kcal/mol) and Coulombic energy (-207.11 kcal/mol) values, indicating robust hydrophobic and electrostatic interactions. Additionally, its XP H-bond score (-3.25 kcal/mol) suggests effective hydrogen bonding with key active site residues. Compound 6 also demonstrated a promising interaction profile, showing the highest van der Waals contribution (-45.35 kcal/mol) and the most negative Coulombic energy (-218.46 kcal/mol), reflecting its deep accommodation into the binding pocket. Its XP H-bond value (-4.18 kcal/mol) was the strongest among all compounds, suggesting significant hydrogen bonding interactions. Though its Glide score (-10.20 kcal/mol) was slightly higher than Compound 1, the overall docking energy and e-model values support its potential as a strong binder. Compounds 2 through 5 also showed better Glide scores than the co-crystal, indicating improved binding affinity. Specifically, Compound 2 had a Glide score of-10.38 kcal/mol and demonstrated a balanced interaction profile with favorable Coulombic energy (-184.07 kcal/mol) and docking energy (-37.48 kcal/mol). Compound 3, despite having a less favorable XP H-bond score (-0.75 kcal/mol), showed considerable van der Waals interactions (-29.92 kcal/mol), suggesting its binding was largely driven by hydrophobic contacts. Compound 4 showed the most negative van der Waals energy (-36.37 kcal/mol) among Compounds 2–5, contributing to a strong

Glide score of-10.15 kcal/mol. Compound 5 displayed a balanced interaction pattern with both hydrophobic and electrostatic contributions, reflected in its Coulombic energy (-185.03 kcal/mol) and XP H-bond score (-2.82 kcal/mol). Compounds 7 to 9, while exhibiting lower Glide scores compared to other designed ligands, still performed comparably or better than the co-crystal. Notably, Compound 8 displayed strong van der Waals interactions (-44.67 kcal/mol) and a Glide score of-9.67 kcal/mol, indicating potential as a lead molecule. In conclusion, most of the designed compounds displayed better docking scores and interaction energies than the co-crystallized ligand, indicating their strong binding affinity toward the SADDL active site. Compounds 1 and 6, in particular, emerged as the most promising candidates for further *in vitro* and *in vivo* validation as potential inhibitors of SADDL.

Binding free energy contributions using MM-GBSA

The binding free energy (ΔG_bind) values for each novel compound within SADDLprotein crystal structure (PDB ID: 2I80) are summarized in table 2. These values were calculated using the MM-GBSA method. The energy components contributing to ΔG_bind include Coulombic energy (ΔG_Coul), hydrophobic energy (ΔG_Lip), hydrogen bonding energy (ΔG_HB), and van der Waals energy (ΔG_VdW).

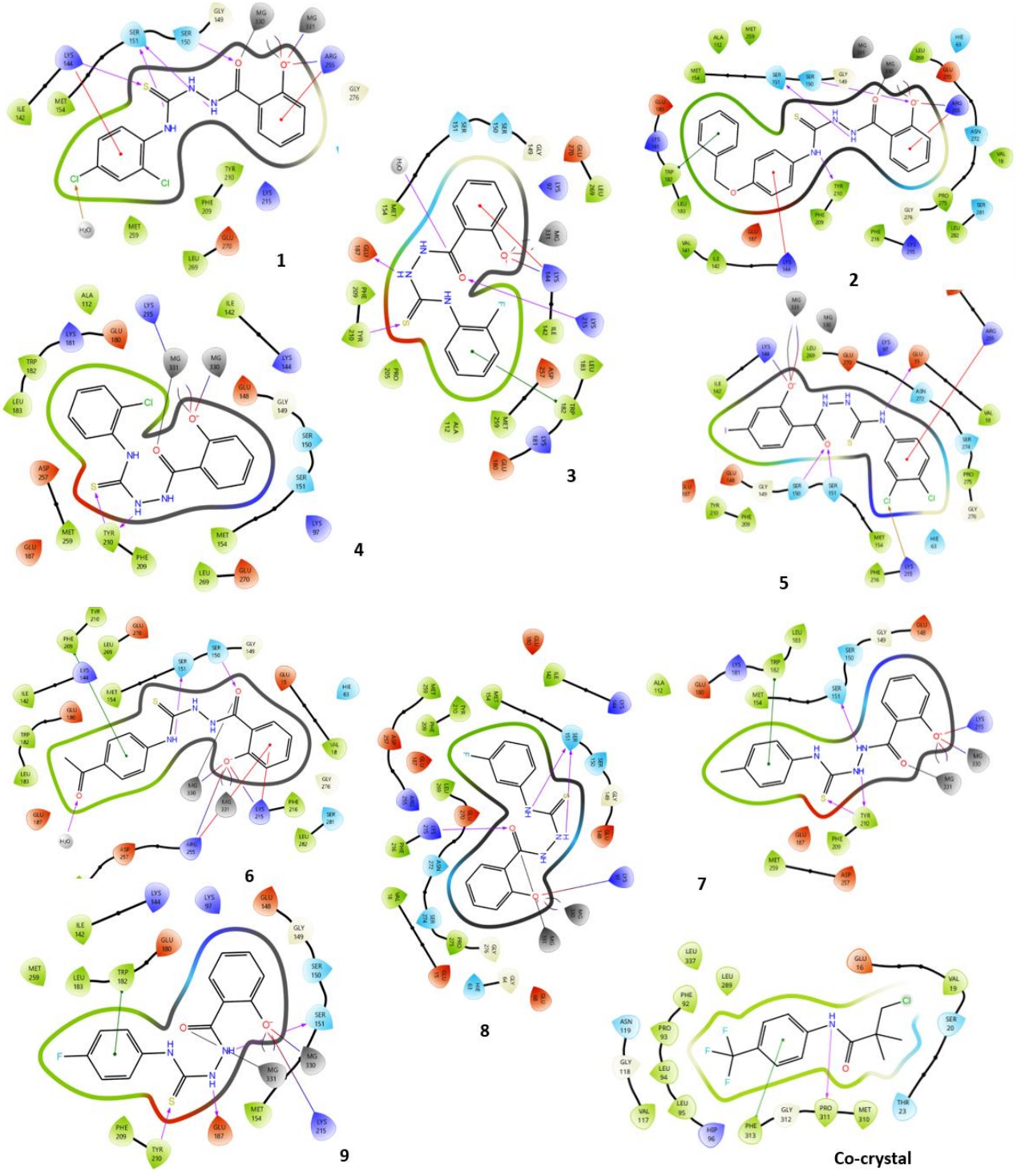

Fig. 1: Compounds (1-9) and co-crystal 2D Interaction Diagrams in the catalytic domain of (SADDL) protein crystal structure (PDB ID: 2I80)

Table 2: Binding free energy (MM-GBSA) contribution (kcal/mol) for the catalytic domain of (SADDL) protein crystal structure (PDB ID: 2I80)

Comp	Glide Bind	Glide Coul	GlideCov	Glide Hb	Glide Lipo	Glide Solv	Glide Vdw	Glide energy
1	-96.06	-31.21	13.90	-0.01	-2.02	15.59	-15.45	14.59
2	-41.57	-40.43	13.97	-1.38	-0.62	4.55	-36.21	10.86
3	-76.66	-38.45	5.71	-0.71	-0.71	1.52	-18.84	6.16
4	-43.22	-6.89	12.77	-0.37	-3.32	7.48	-30.05	0.85
5	-49.81	-12.23	7.23	-0.87	-1.50	1.08	-40.22	3.72
6	-45.96	-41.29	5.22	-1.71	-0.48	6.94	-19.11	13.33
7	-40.46	-33.21	15.90	-2.01	-1.02	18.59	-17.45	16.59
8	-81.95	-42.43	15.97	-3.38	-1.52	6.55	-38.21	12.86
9	-41.95	-40.45	7.71	-2.71	-1.61	3.52	-20.84	8.16
co-crystal	-59.98	-13.29	2.36	-0.30	-16.20	18.22	-18.05	3.25

[a]Free Energy of Binding, [b]Coulomb Energy, [c]Hydrogen Bonding Energy, [d]Hydrophobic Energy (non-polar contribution estimated by solvent accessible surface area), [e]Van der Waals Energy.

Among all compounds, Compound 1 demonstrated the most favorable binding energy (ΔG_bind =-96.06 kcal/mol), which is significantly lower than the co-crystal ligand (-59.98 kcal/mol). This strong binding can be attributed to its optimal van der Waals interactions (-15.45 kcal/mol), Coulombic contribution (-31.21 kcal/mol), and minimal solvation penalty (+15.59 kcal/mol), reflecting stable interactions within the active site. Compound 8 also exhibited a highly favorable ΔG_bind of-81.95 kcal/mol, supported by strong electrostatic energy (-42.43 kcal/mol) and van der Waals energy (-38.21 kcal/mol), surpassing the co-crystal. Its substantial hydrogen bonding energy (-3.38 kcal/mol) further confirms strong polar interactions within the binding pocket. Compound 3 showed a ΔG_bind of-76.66 kcal/mol, with moderate electrostatic and van der Waals contributions, suggesting stable binding despite limited hydrogen bond formation. Similarly, Compound 5 (-49.81 kcal/mol) and Compound 6 (-45.96 kcal/mol) displayed favorable profiles, though slightly less than the reference ligand. Interestingly, Compound 2 showed a comparatively lower ΔG_bind (-41.57 kcal/mol), despite high electrostatic interaction (-40.43 kcal/mol), likely due to the unfavorable solvation energy (+4.55 kcal/mol). Compound 4 and Compound 7 also showed less negative ΔG_bind values (-43.22 and-40.46 kcal/mol, respectively), indicating moderate affinity. Compound 9, with a ΔG_bind of-41.95 kcal/mol, had balanced Coulombic and van der Waals interactions, but a higher solvation penalty and moderate hydrogen bonding contributed to its lower overall affinity. In comparison, the co-crystallized ligand showed a ΔG_bind of-59.98 kcal/mol, with strong lipophilic contributions (-16.20 kcal/mol) and moderate van der Waals energy (-18.05 kcal/mol). However, most of the designed compounds—particularly Compounds 1, 8, and 3—demonstrated superior binding free energies, reinforcing their potential as stronger inhibitors.

Fig. 1 illustrates the 2D interaction diagrams of nine novel compounds, detailing their binding within the catalytic domain of the Staphylococcus aureus D-alanine: D-alanine ligase (SADDL) protein (PDB ID: 2I80). The diagrams highlight key molecular interactions, including hydrogen bonds formed between functional groups-such as amines (NH), carbonyl (C=O), thiocarbonyl group (C=S), and oxygen atoms-and active site residues like TYR210, SER151, LYS215, GLU187, SER150, and GLU15. Additionally, π–π stacking interactions are observed between the aromatic rings of the compounds and aromatic residues TRP182 and PHE209. π–cation interactions are also evident between the ligand's aromatic rings and positively charged residues LYS144 and ARG255. These diagrams provide a clear visualization of how specific functional groups contribute to the stabilization and effective binding of the compounds to the SADDL active site.

MD simulation study

The docking pose of the ligand N-(3,4-dichlorophenyl)-2-(2-hydroxybenzoyl) hydrazine-1-carboxamide (Compound 1/2I80) was analyzed through 100 ns MD simulations. Along with a 2D interaction diagram, the study provided detailed insights into several parameters, including protein–ligand interaction fractions, timing of binding contacts, RMSD, and RMSF.

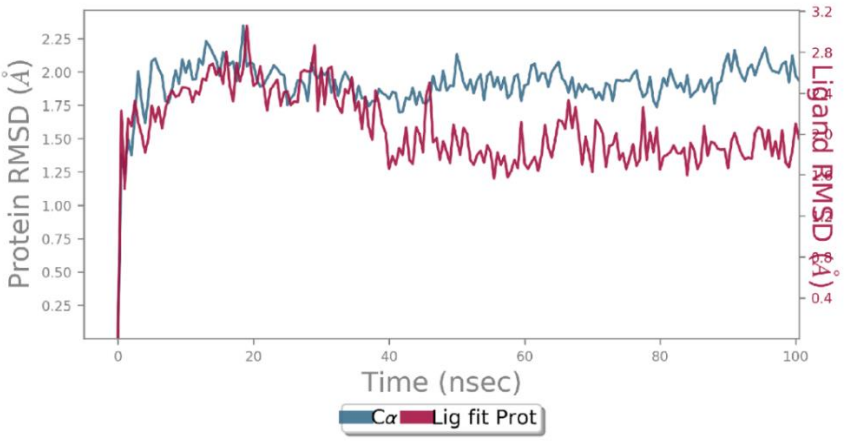

Fig. 2: RMSD for compound 1/2I80 protein-ligand complex

The RMSD analysis of the Cα atoms for the ligand's docking pose ranged from 1.20 to 2.0 Å during the initial 0–40 ns, indicating moderate stability.

Between 40 and 100 ns of the simulation, the ligand remained stably bound within the active site, with RMSD values ranging from 1.30 to 2.80 Å, indicating maintained structural stability of the protein–ligand complex. Overall, the ligand's Cα atoms remained stable for approximately 60 ns throughout the 100 ns simulation.

Similarly, the ligand's fit to the protein showed stability for about 60 ns, with moderate consistency in the first 40 ns (RMSD: 1.30 to 2.7 Å) and continued stability during 40–100 ns, within a range of 1.50 to 2.8 Å. These results are visually represented in fig. 2.

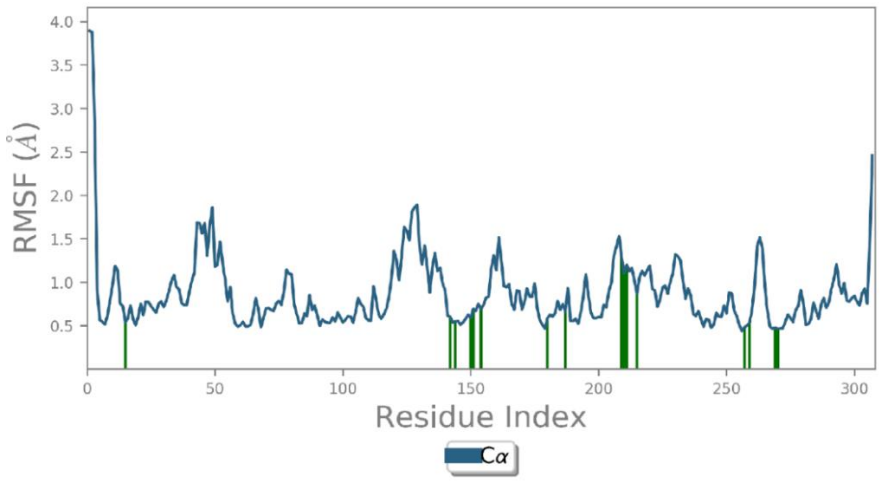

Fig. 3: RMSF for compound 1/2I80 protein-ligand complex

The RMSF analysis, as shown in fig. 3, revealed minimal fluctuations throughout the simulation. The Cα atoms exhibited initial variations ranging from 0.5 to 2.0 Å but remained largely stable over time. Minor fluctuations were observed in specific time intervals, particularly between 149–153 ns, 180–220 ns, and 250–270 ns. During these periods, the RMSF values for the amino acid residues ranged from 0.5 to 1.0 Å, 0.5 to 1.8 Å, and 0.5 to 1.5 Å, respectively. These results indicate that the ligand–protein complex maintained structural stability with only slight local flexibility in certain regions.

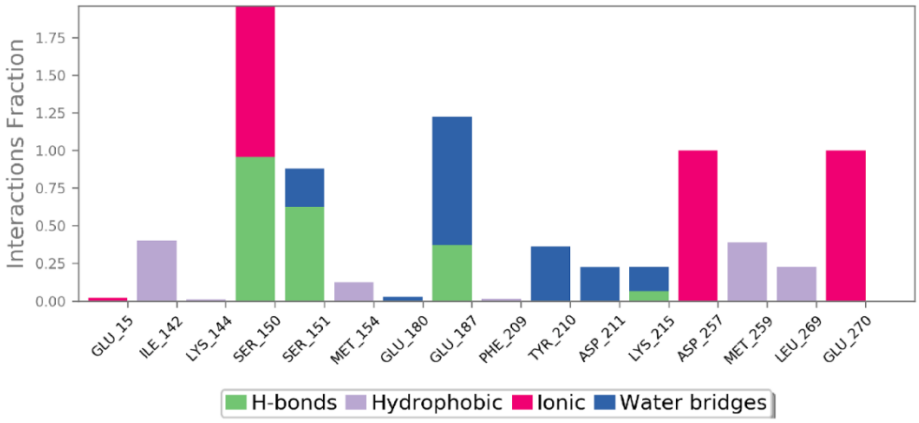

Fig. 4: Protein-ligand contacts for compound 1/2I80 protein-ligand complex

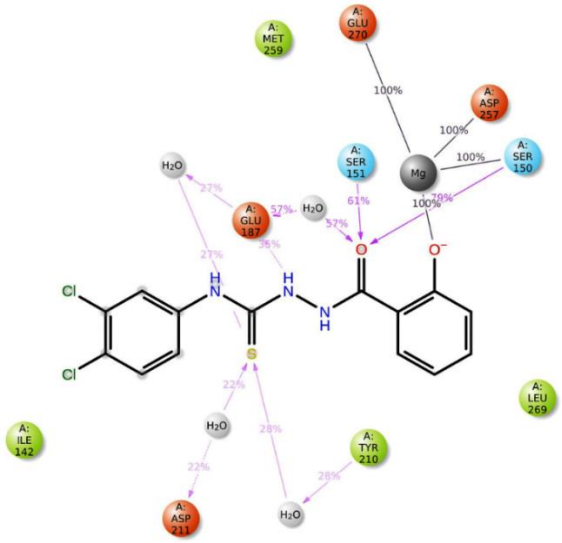

Fig. 5: 2D diagram for compound 1/2I80protein-ligand complex

Fig. 4 illustrates the range of interactions between the ligand and amino acid residues, including ionic bonds, hydrophobic contacts, and water bridge interactions. While some interactions such as ionic, hydrophobic, and water bridges were observed, their individual stability percentages were relatively low: hydrophobic interactions with Ile142, Lys144, and Met154 showed a stability of 0.0% out of 0.40%; water bridges with Glu180, Tyr210, Met254, and Leu269 maintained 0.0% out of 0.50%; and ionic bonds with Glu270, Asp257, Asp211, and Glu15 were maintained at 0.0% out of 1.0%. However, the ligand demonstrated strong and consistent binding with key residues Ser150, Ser151, Glu187, and Lys215, maintaining a full interaction stability of 1.75%. These results emphasize the importance of these specific residues in stabilizing the ligand–receptor complex.

Fig. 5 displays the 2D interaction diagram of the protein–ligand contacts for compound 1. Metal coordination plays a significant role, with residues Glu270, Asp257, and Ser150 forming stable interactions between the ligand's oxygen group and the magnesium ion, maintaining 100% interaction stability. Ser151 consistently forms a hydrogen bond with the ligand's carbonyl group, exhibiting 61% stability. Similarly, Asp211 interacts with the sulfonyl group via a hydrogen bond, showing 22% stability. Additionally, Glu187 forms a hydrogen bond with the ligand's amide group, with a stability of 35%. These findings suggest that compound 1 shows strong and specific binding interactions with the SADDL active site, highlighting its potential as a promising lead for the development of new anti-SADDL agents.

DISCUSSION

The present study focused on identifying novel inhibitors targeting Staphylococcus aureus D-alanine: D-alanine ligase (SADDL), a key enzyme in bacterial cell wall biosynthesis. Among the designed molecules, Compound 1 demonstrated superior binding affinity, with a Glide score of-11.11 kcal/mol, notably outperforming the co-crystallized reference ligand (-9.88 kcal/mol). However, it is important to emphasize that Glide scores represent computational predictions and do not reflect experimentally validated potency. Without *in vitro* data such as Minimum Inhibitory Concentration (MIC) or IC_{50} values, these results should be interpreted with caution.

These findings are in line with earlier reports emphasizing the importance of targeting SADDL to develop potent antibacterial agents [43]. Previous studies have reported Glide scores ranging from-8.0 to-9.5 for known DDL inhibitors, whereas Compound 1 in the current study showed significantly better binding characteristics. The strong van der Waals and Coulombic interactions, along with stable hydrogen bonding with active site residues (Ser151, Glu187, Asp211), are consistent with the binding profiles reported for efficient SADDL inhibitors [44]. The observed stable binding in MD simulations over 100 ns, with minimal RMSD and RMSF deviations, further supports the robustness of Compound 1 as a lead candidate. Furthermore, Compound 6 exhibited the highest van der Waals and Coulombic contributions, correlating well with similar structural analogs documented for their high lipophilic binding energy in prior studies. Compound 8 also showed favorable electrostatic and hydrophobic interactions, making it a potential secondary lead. These findings resonate with earlier computational studies where similar hydrophobic and electrostatic profiles were linked to enhanced ligand binding and antibacterial efficacy. Importantly, the involvement of metal coordination with Mg^{2+} ions observed in the MD simulations of Compound 1 underscores the relevance of metal–ligand interactions in DDL inhibition, a feature highlighted in other studies focusing on the enzymatic catalytic mechanism [45]. The overall performance of Compounds 1, 6, and 8 positions them as promising candidates for further *in vitro* and *in vivo* validation. These computational findings contribute to the growing body of research aimed at targeting bacterial D-alanine: D-alanine ligases and offer promising leads that surpass some previously reported candidates in binding efficiency and stability. Continued efforts in synthesis and biological evaluation are necessary to confirm the therapeutic potential of these molecules as novel antibacterial agents.

CONCLUSION

Molecular docking and MD simulations revealed that several designed compounds exhibited stronger binding to Staphylococcus aureus D-alanine: D-alanine ligase (SADDL) than the co-crystallized ligand. Compound 1 showed the best results with a Glide score of-11.11 kcal/mol and binding free energy ΔG_bind-96.06 kcal/mol, which is significantly better than the reference ligand (-59.98 kcal/mol). It formed strong van der Waals, Coulombic, and hydrogen bond interactions with active site residues like Ser150, Ser151, Glu187, and Lys215. Compound 6 had the highest van der Waals and Coulombic contributions and the best XP H-bond score, while Compound 8 (Glide score:-9.67, ΔG_bind:-81.95 kcal/mol) showed promising electrostatic and hydrophobic interactions. MD simulation of Compound 1 confirmed stable binding over 100 ns, with consistent RMSD/RMSF and stable interactions, including magnesium coordination and key hydrogen bonds. Overall, Compound 1 is the most promising SADDL inhibitor, with Compounds 6 and 8 also showing potential for further *in vitro* and *in vivo* studies.

ACKNOWLEDGMENT

The authors would like to thank the Department of Pharmaceutical Chemistry, JSS College of Pharmacy, Ooty, Tamil Nadu, for providing facilities for conducting the Research.

FUNDING

No funding was received for this work.

AUTHORS CONTRIBUTIONS

Abisha Thomas - Conceptualization, validation, original draft preparation, and data curation. Dr. Md. Afzal Azam-Data curation, methodology, and writing-review and editing.

CONFLICT OF INTERESTS

Declared none

REFERENCES

1. Silver LL. Multi-targeting by monotherapeutic antibacterials. Nat Rev Drug Discov. 2007;6(1):41-55. doi: 10.1038/nrd2202, PMID 17159922.
2. Boucher HW, Talbot GH, Bradley JS, Edwards JE, Gilbert D, Rice LB. Bad bugs no drugs: no ESKAPE! an update from the infectious diseases society of America. Clin Infect Dis. 2009;48(1):1-12. doi: 10.1086/595011, PMID 19035777.
3. Wong KK, Pompliano DL. Peptidoglycan biosynthesis. Unexploited antibacterial targets within a familiar pathway. Adv Exp Med Biol. 1998;456:197-217. doi: 10.1007/978-1-4615-4897-3_11, PMID 10549370.
4. Prosser GA, De Carvalho LP. Kinetic mechanism and inhibition of mycobacterium tuberculosis D-alanine:D-alanine ligase by the antibiotic D-cycloserine. FEBS Journal. 2013;280(4):1150-66. doi: 10.1111/febs.12108, PMID 23286234.
5. Hrast M, Vehar B, Turk S, Konc J, Gobec S, Janezic D. Function of the D-alanine:D-alanine ligase lid loop: a molecular modeling and bioactivity study. J Med Chem. 2012;55(15):6849-56. doi: 10.1021/jm3006965, PMID 22803830.
6. Zawadzke LE, Bugg TD, Walsh CT. Existence of two D-alanine: D-alanine ligases in escherichia coli: cloning and sequencing of the ddlA gene and purification and characterization of the DdlA and DdlB enzymes. Biochemistry. 1991;30(6):1673-82. doi: 10.1021/bi00220a033, PMID 1993184.
7. Tytgat I, Colacino E, Tulkens PM, Poupaert JH, Prevost M, Van Bambeke F. DD-ligases as a potential target for antibiotics: past present and future. Curr Med Chem. 2009;16(20):2566-80. doi: 10.2174/092986709788682029, PMID 19601798.
8. Wright GD, Walsh CT. D-alanyl-D-alanine ligases and the molecular mechanism of vancomycin resistance. Acc Chem Res. 1992;25(10):468-73. doi: 10.1021/ar00022a006.
9. Arthur M, Reynolds P, Courvalin P. Glycopeptide resistance in enterococci. Trends Microbiol. 1996;4(10):401-7. doi: 10.1016/0966-842X(96)10063-9, PMID 8899966.
10. Fan C, Park IS, Walsh CT, Knox JR. D-alanine:D-alanine ligase: phosphonate and phosphinate intermediates with wild type and the Y216F mutant. Biochemistry. 1997;36(9):2531-8. doi: 10.1021/bi962431t, PMID 9054558.

11. Liu S, Chang JS, Herberg JT, Horng MM, Tomich PK, Lin AH. Allosteric inhibition of staphylococcus aureus D-alanine:D-alanine ligase revealed by crystallographic studies. Proc Natl Acad Sci USA. 2006;103(41):15178-83. doi: 10.1073/pnas.0604905103, PMID 17015835, PMCID PMC1622796.
12. Duncan K, Walsh CT. ATP-dependent inactivation and slow binding inhibition of salmonella typhimurium D-alanine: D-alanine ligase (ADP) by (aminoalkyl)phosphinate and aminophosphonate analogues of D-alanine. Biochemistry. 1988;27(10):3709-14. doi: 10.1021/bi00410a028, PMID 3044448.
13. Knox JR, Moews PC, Fan C. Complex of D-ala: D-ala ligase with ADP and a phosphoryl phosphonate. Biochemistry. 1997;36:2531. doi: 10.2210/pdb1IOV/pdb.
14. Putty S, Rai A, Jamindar D, Pagano P, Quinn CL, Mima T. Characterization of d-boroAla as a novel broad spectrum antibacterial agent targeting d-Ala-d-Ala ligase. Chem Biol Drug Des. 2011;78(5):757-63. doi: 10.1111/j.1747-0285.2011.01210.x, PMID 21827632.
15. Prosser GA, De Carvalho LP. Reinterpreting the mechanism of inhibition of mycobacterium tuberculosis D-alanine:D-alanine ligase by D-cycloserine. Biochemistry. 2013;52(40):7145-9. doi: 10.1021/bi400839f, PMID 24033232.
16. Lu Y, Xu H, Zhao X. Crystal structure of the Apo form of D-alanine:D-alanine ligase (DDl) from streptococcus mutans. Protein Pept Lett. 2010;17(8):1053-7. doi: 10.2174/092986610791498858, PMID 20522004.
17. Batson S, Majce V, Lloyd AJ, Rea D, Fishwick CW, Simmons KJ. The X-ray crystal structure of D-alanyl-D-alanine ligase in complex with ATP and D-ala-D-ala. Nat. Commun. 2017;8:1939.
18. Fan C, Park IS, Walsh CT, Knox JR. D-alanine: D-alanine ligase: phosphonate and phosphinate intermediates with wild type and the Y216F mutant. Biochemistry. 1997;36(9):2531-8. doi: 10.1021/bi962431t, PMID 9054558.
19. Fan C, Moews PC, Walsh CT, Knox JR. Vancomycin resistance: structure of D-alanine:D-alanine ligase at 2.3 a resolution. Science. 1994;266(5184):439-43. doi: 10.1126/science.7939684, PMID 7939684.
20. Shi Y, Walsh CT. Active site mapping of escherichia coli d-Ala-d-Ala ligase by structure based mutagenesis. Biochemistry. 1995;34(9):2768-76. doi: 10.1021/bi00009a005, PMID 7893688.
21. Elassal ES, Fahmy AO, Saad AN, Ali AH, Elshenety AH, Badr OA. Discovery and development of new antibacterial drugs. In: microbial genomics: clinical pharmaceutical and industrial applications. Amsterdam: Elsevier. 2024. p. 333-59. doi: 10.1016/B978-0-443-18866-4.00012-2.
22. Lee JH, Na Y, Song HE, Kim D, Park BH, Rho SH. Crystal structure of the apo form of D-alanine: D-alanine ligase (DDL) from thermus caldophilus: a basis for the substrate induced conformational changes. Proteins. 2006;64(4):1078-82. doi: 10.1002/prot.20927, PMID 16779845.
23. Parsons WH, Patchett AA, Bull HG, Schoen WR, Taub D, Davidson J. Phosphinic acid inhibitors of D-alanyl-D-alanine ligase. J Med Chem. 1988;31(9):1772-8. doi: 10.1021/jm00117a017, PMID 3137344.
24. Chakravarty PK, Greenlee WJ, Parsons WH, Patchett AA, Combs P, Roth A. (3-Amino-2-oxoalkyl)phosphonic acids and their analogues as novel inhibitors of D-alanine:D-alanine ligase. J Med Chem. 1989;32(8):1886-90. doi: 10.1021/jm00128a033, PMID 2502630.
25. Lacoste A, Chollet Gravey A, Vo Quang L, Vo Quang Y, Le Goffic F. Time-dependent inhibition of streptococcus faecalisd alanine: d-alanine ligase by α-aminophosphonamidic acids. Eur J Med Chem. 1991;26(3):255-60. doi: 10.1016/0223-5234(91)90057-T.
26. Paymal SB, Barale SS, Supanekar SV, Sonawane KD. Structure based virtual screening molecular dynamic simulation to identify the oxadiazole derivatives as inhibitors of enterococcus D-Ala-D-Ser ligase for combating vancomycin resistance. Comput Biol Med. 2023 Jun 1;159:106965. doi: 10.1016/j.compbiomed.2023.106965, PMID 37119552.
27. Walker EH, Walker EH, Pacold ME, Perisic O, Stephens L, Hawkins PT, Wymann MP. Structural determinants of phosphoinositide 3-kinase inhibition by wortmannin LY294002, quercetin myricetin and staurosporine. Mol Cell. 2000;6(4):909-19. doi: 10.1016/s1097-2765(05)00089-4, PMID 11090628.
28. Baqi MA, Jayanthi K, Rajeshkumar R. Molecular docking insights into probiotics sakacin p and sakacin a as potential inhibitors of the cox-2 pathway for colon cancer therapy. Int J App Pharm. 2025;17(1):153-60. doi: 10.22159/ijap.2025v17i1.52476.
29. Pant K, Karpel RL, Rouzina I, Williams MC. Mechanical measurement of single molecule binding rates: kinetics of DNA helix-destabilization by T4 gene 32 protein. J Mol Biol. 2004;336(4):851-70. doi: 10.1016/j.jmb.2003.12.025, PMID 15095865.
30. Sherman W, Beard HS, Farid R. Use of an induced fit receptor structure in virtual screening. Chem Biol Drug Des. 2006 Jan;67(1):83-4. doi: 10.1111/j.1747-0285.2005.00327.x, PMID 16492153.
31. Redhu S, Jindal A. Molecular modelling: a new scaffold for drug design. Int J Pharm Pharm Sci. 2013;5 Suppl 1:5-8.
32. Shaikh SI, Zaheer Z, Mokale SN, Lokwani DK. Development of new pyrazole hybrids as antitubercular agents: synthesis biological evaluation and molecular docking study. Int J Pharm Pharm Sci. 2017;9(10):50-6. doi: 10.22159/ijpps.2017v9i11.20469.
33. Friesner RA, Banks JL, Murphy RB, Halgren TA, Klicic JJ, Mainz DT. Glide: a new approach for rapid accurate docking and scoring. 1. Method and assessment of docking accuracy. J Med Chem. 2004 Mar 1;47(7):1739-49. doi: 10.1021/jm0306430, PMID 15027865.
34. Jayanthi K, Ahmed SS, Baqi MA, Afzal Azam MA. Molecular docking dynamics of selected benzylidene aminophenyl acetamides AsTmk inhibitors using high throughput virtual screening (Htvs). Int J App Pharm. 2024;16(3):290-7. doi: 10.22159/ijap.2024v16i3.50023.
35. Humphrey W, Dalke A, Schulten K. VMD: visual molecular dynamics. J Mol Graph. 1996 Feb 1;14(1):33-8. doi: 10.1016/0263-7855(96)00018-5, PMID 8744570.
36. Qin Y, Xu L, Teng Y, Wang Y, Ma P. Discovery of novel antibacterial agents: recent developments in D-alanyl-D-alanine ligase inhibitors. Chem Biol Drug Des. 2021 Sep;98(3):305-22. doi: 10.1111/cbdd.13899, PMID 34047462.
37. Kovac A, Konc J, Vehar B, Bostock JM, Chopra I, Janezic D. Discovery of new inhibitors of D-alanine: D-alanine ligase by structure based virtual screening. J Med Chem. 2008 Dec 11;51(23):7442-8. doi: 10.1021/jm800726b, PMID 19053785.
38. Pauza NL, Cotti MP, Godar L, De Sancovich AF, Sancovich HA. Disturbances on delta aminolevulinate dehydratase (ALA-D) enzyme activity by Pb_2+ Cd_2, Cu_2, Mg_2, Zn_2, Na+, K+and Li+: analysis based on coordination geometry and acid base lewis capacity. J Inorg Biochem. 2005 Feb 1;99(2);409-14. doi: 10.1016/j.jinorgbio.2004.10.013, PMID 15621272.